Few Body Systems manuscript No.
(will be inserted by the editor)

D. Blaschke · J. Berdermann · J. Cleymans · K. Redlich

Chiral condensate and Mott-Anderson freeze-out

arXiv:1109.5391v1 [hep-ph] 25 Sep 2011

Received: date / Accepted: date

Abstract We present the idea of a Mott-Anderson freeze-out that suggests a key role of the localization of the hadron wave functions when traversing the hadronization transition. The extension of hadron wave functions in dense matter is governed by the behavior of the chiral quark condensate such that its melting at finite temperatures and chemical potentials entails an increase of the size of hadrons and thus their geometrical strong interaction cross sections. It is demonstrated within a schematic resonance gas model, that a kinetic freeze-out condition reveals a correlation with the reduction of the chiral condensate in the phase diagram up to 50% of its vacuum value. Generalizing the description of the chiral condensate by taking into account a full hadron resonance gas such correlation gets distorted. We discuss, that this may be due to our approximations in calculating the chiral condensate which disregard both, in-medium effects on hadron masses and hadron-hadron interactions. The latter, in particular due to quark exchange reactions, could lead to a delocalization of the hadron wave functions in accordance with the picture of a Mott-Anderson transition.

Keywords Chiral condensate · chemical freeze-out · Mott-Anderson transition

1 Introduction

The investigation of the structure of the QCD phase-diagram is one of the goals of heavy-ion collision experiments as well as theoretical studies within lattice QCD (LQCD) and effective field theory approaches to the non-perturbative sector of QCD. Of particular interest are the conditions under which the approximate chiral symmetry of the QCD Lagrangian get restored and whether this transition is to be necessarily accompanied by the deconfinement of quarks and gluons. More detailed questions to the QCD phase transitions concern their order, their critical exponents as well as the existence of a

Presented at the workshop "30 years of strong interactions", Spa, Belgium, 6-8 April 2011.

D. Blaschke
Institute for Theoretical Physics, University of Wroclaw, 50-204 Wroclaw, Poland
Bogoliubov Laboratory of Theoretical Physics, JINR, 141980 Dubna, Russia
Tel.: +48-71-375 9252
Fax: +48-71-321 4454
E-mail: blaschke@ift.uni.wroc.pl

J. Berdermann
DESY Zeuthen, D-15738 Zeuthen, Germany

J. Cleymans
UCT-CERN Research Centre and Department of Physics, Rondebosch 7701, Cape Town, South Africa

K. Redlich
Institute for Theoretical Physics, University of Wroclaw, 50-204 Wroclaw, Poland
ExtreMe Matter Institute EMMI, GSI, D-64291 Darmstadt, Germany

critical point or even a triple point in the phase diagram. Most promising tools for the experimental determination of these characteristics are the energy scan programs at CERN, RHIC and at the upcoming dedicated facilities of the third generation: FAIR and NICA. The systematic analysis of higher moments of distributions of produced particles in their dependence on the collision energy and the size of colliding systems shall provide answers to the above questions and allow for direct comparison with predictions from the underlying theory, as provided by LQCD, see, e.g., Ref. [1].

As long as the applicability of LQCD methods is bound to the region of finite T and $\mu_B/T \ll 1$, any predictions for the phase structure of QCD at high baryon densities including the possible existence of critical points will rely on effective models. To be relevant for the discussion of the above problems these models have to share with QCD the property of chiral symmetry and its dynamical breaking as well as a mechanism for confinement and deconfinement.

At present, the position of (pseudo-)critical lines in the QCD phase diagram is constrained by the chemical freeze-out parameters (T^f, μ_B^f) which have been obtained from the statistical model analysis of particle yields obtained in heavy ion collisions [2; 3]. One of the most striking observations is the systematic behaviour of these parameters with collision energy $\sqrt{s}$ [4; 5; 6], which has recently been given a simple parametric form [7]. It has been observed, that the resulting freeze-out curve in the phase diagram is closely correlated to the thermodynamical quantities of the hadron resonance gas described by the statistical model, see Fig. 1. These phenomenological freeze-out conditions make statements about the mean energy per hadron $\langle E\rangle/\langle N\rangle \simeq 1.0$ GeV, the dimensionless entropy density $s/T^3 \simeq 7$ and a total baryon and antibaryon density $n_B + n_{\bar{B}} \simeq 0.12$ fm^{-3}. The freeze-out line provides a lower bound for the chiral restoration and deconfinement transitions in the phase diagram. Being coincident at low densities as inferred from LQCD [8], both transitions need not to occur simultaneously at high densities, thus allowing for an island of a quarkyonic phase [9] between hadron gas and quark-gluon plasma with a (pseudo-)triple point [10]. The question appears for the physical mechanism which

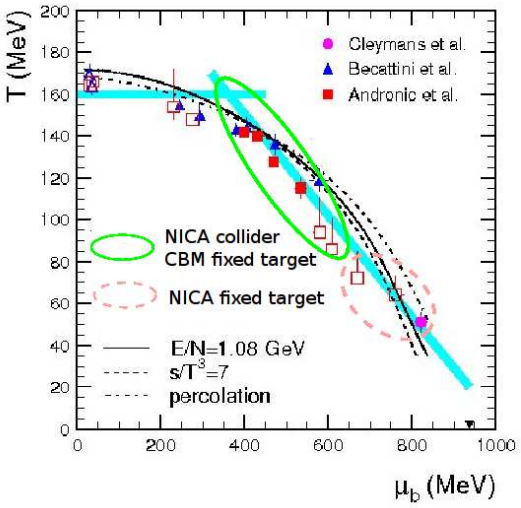

Fig. 1 Freeze-out parameters from the statistical model [10] compared to phenomenological rules for explaining their systematics in the temperature - chemical potential plane. Ellipses indicate regions where dedicated future experiments (FAIR-CBM and JINR-NICA) could provide new data for more detailed investigations.

governs the chemical freeze-out and which determines quantitatively the freeze-out parameters. One aspect is provided by the requirement that hadrons should overlap in order to facilitate flavor exchange reactions which establish chemical equilibrium. This geometrical picture of freeze-out is successfully realized in a percolation theory approach [11]. Another aspect is the dynamical one: when the equation of state (EoS) possess softest points (e.g., due to the dissociation of hadrons into their quark and gluon constituents with a sufficient release of binding energy involved) which is correlated with the freeze-out

curve in the phase diagram, then it is expected that the hadron abundances are characterized by the corresponding T and μ_B values [12]. The dynamical system got quasi trapped at the softest points for sufficient time to achieve chemical equilibration before evaporating as a gas of hadron resonances freely streaming to the particle detectors. Also the kinetic aspect of fast chemical equilibration was discussed in the hadronic gas when accounting for a multi-hadron dynamics [13].

All these mechanisms are appealing since they provide an intuitively clear picture, but they are flawed by the fact that their relation to fundamental aspects of the QCD phase transition like the chiral condensate as an order parameter are not an element of the description.

In the present contribution we develop an approach which relates the geometrical as well as the hydrodynamic and kinetic aspects of chemical freeze-out to the medium dependence of the chiral condensate. We demonstrate within a beyond-meanfield extension [14; 15; 16; 17; 18; 19] of the Polyakov NJL model [20; 21; 22; 23] how the excitation of hadronic resonances initiates the melting of the chiral condensate which entails a Mott-Anderson type delocalization [24; 25; 26] of hadron wave functions at the hadronic to quark matter phase transition [27]. Already for a schematic resonance gas consisting of pions and nucleons with artificially enhanced numbers of degrees of freedom we can demonstrate that a kinetic freeze-out condition for the above model provides quantitative agreement with the phenomenological freeze-out curve.

We propose a generalization of this approach by including a more complete description of the chiral condensate which accounts for contributions from the hadron resonance gas and the chiral dynamics implemented from the PNJL model. We demonstrate, that in this approach correlations between freeze-out and chiral condensate get distorted. We discuss, that this may be due to our approximations which exclude the in-medium effects on hadron masses as well as the hadron-hadron interactions which could result in delocalization of the hadron wave functions in accordance with the picture of a Mott-Anderson transition.

2 Mott-Anderson freeze-out and chiral condensate

Recently, we have suggested, that the chemical freeze–out in heavy ion collisions can be linked to the chiral condensate [28]. The starting point is based on the assumption, that the chemical freeze–out sets in if the collision and the expansion time are equal. Thus, in the temperature-chemical potential (T, μ)-plane, the kinetic freeze-out condition is formulated as

$$\tau_{\rm exp}(T,\mu) = \tau_{\rm coll}(T,\mu) \ , \tag{1}$$

where $\tau_{\rm exp}(T,\mu)$ is the expansion time of the hadronic fireball, and

$$\tau_{\rm coll}^{-1}(T,\mu) = \sum_{i,j} \sigma_{ij} n_j \ , \tag{2}$$

is the inverse relaxation time for reactive collisions with $i, j = \pi, N, ...$ running over all particle species in the hadron resonance gas. For the hadron-hadron cross sections σ_{ij} we adopt the geometrical Povh-Hüfner law, [29; 30]

$$\sigma_{ij} = \lambda \langle r_i^2 \rangle \langle r_j^2 \rangle \ , \tag{3}$$

where λ is a constant, being of the order of the string tension, $\lambda \sim 1$ GeV/fm $= 5$ fm^{-2}. Note, that this behavior was also obtained for the quark exchange contribution to hadron-hadron cross sections [31].

A key point of our approach is that the radii of hadrons depend on T and μ and that they diverge, when hadron dissociation (Mott-Anderson delocalization) driven basically by the restoration of the chiral symmetry, sets in. This has been quantitatively studied for the pion [32], where it has been shown, that close to the Mott-Anderson transition the pion radius is well approximated by

$$r_\pi^2(T,\mu) = \frac{3}{4\pi^2} F_\pi^{-2}(T,\mu) \ . \tag{4}$$

In addition, it has been demonstrated, that the GMOR relation holds out to the chiral phase transition, where pions merge the continuum of unbound quark matter [33; 34]. Furthermore, since the

current-quark mass is $T-$ and $\mu-$independent and the pion mass is "chirally protected", the $T-$ and $\mu-$dependence of the chiral condensate should be similar to that of the pion decay constant,

$$F_\pi^2(T,\mu) = -m_0\langle\bar{q}q\rangle_{T,\mu}/m_\pi^2. \tag{5}$$

Consequently, the relationship between the pion radius and the chiral condensate reads

$$r_\pi^2(T,\mu) = \frac{3m_\pi^2}{4\pi^2 m_q}|\langle\bar{q}q\rangle_{T,\mu}|^{-1} \ . \tag{6}$$

The Mott-Anderson delocalization of the pion wave function due to melting of the chiral condensate, as expressed in this formula, is the important element of the hadronic freeze-out mechanism suggested in [28].

For the nucleon, we assume that its radius consist of two components; a medium independent hard core radius r_0, and a pion cloud contribution as

$$r_N^2(T,\mu) = r_0^2 + r_\pi^2(T,\mu) \ , \tag{7}$$

where from the vacuum values $r_\pi = 0.59$ fm and $r_N = 0.74$ fm one gets $r_0 = 0.45$ fm.

For the expansion time scale we adopt the relation which follows from the entropy conservation, $S = s(T,\mu)\ V(\tau_{\rm exp}) = {\rm const}$ with $V(\tau_{\rm exp})$ being a fireball volume. Assuming, that $V(\tau_{\rm exp}) \propto \tau_{\rm exp}^3$ one gets

$$\tau_{\rm exp}(T,\mu) = a\ s^{-1/3}(T,\mu) \ , \tag{8}$$

with a being a constant of the order one.

To quantify the freeze-out conditions in the $(T-\mu)$ plane, we first consider a medium which is composed of pions and nucleons only, however, with a variable number of degrees of freedom. In this way, we account effectively for additional mesonic and baryonic stats in the hadron resonance gas. A generalization to a medium composed of all hadrons with physical degrees of freedom will be discussed later.

We start from a medium-modified chiral condensate obtained within the chiral perturbation theory [35; 36],

$$\frac{\langle\bar{q}q\rangle}{\langle\bar{q}q\rangle_{\rm vac}} = 1 - \frac{n_{s,\pi}(T)}{m_\pi F_\pi^2} - \frac{\Sigma_{\pi N} n_{s,N}(T,\mu)}{m_\pi^2 F_\pi^2} \ , \tag{9}$$

where the pion-nucleon sigma-term is $\Sigma_{\pi N} = m_0(\partial m_N/\partial m_0) = 45$ MeV [37], and the scalar densities of pions $n_{s,\pi}$ and nucleons $n_{s,N}$ read

$$n_{s,\pi} = d_\pi \int_0^\infty \frac{dp\,p^2}{2\pi^2}\frac{m_\pi}{E_\pi(p)} f_\pi(E_\pi(p)) \ , \tag{10}$$

$$n_{s,N} = \frac{d_N}{2\pi^2}\int_0^\infty dp\,p^2\,\frac{m_N}{E_N(p)}\left\{f_N^+(E_N(p)) + f_N^-(E_N(p))\right\} \ . \tag{11}$$

with d_π the pionic and d_N the nucleonic number of degrees of freedom. In the chiral limit and for $d_\pi = 3$ we have, $n_{s,\pi}/m_\pi = T^2/8$. Fig. 2 shows the chemical freeze-out lines in the $(T-\mu)$-plane obtained from the kinetic freeze-out conditions (1) for three sets of pion and nucleon degrees of freedom. The best description of the phenomenological freeze-out points is obtained for $d_\pi = 8$ and $d_N = 20$. The inset of Fig. 2 shows a dependence of the position of the freeze-out line on the expansion (solid-line) and the collision (dashed-line) times used in the model for $d_\pi = 8$ and $d_N = 20$.

From Fig. 2 one concludes, that the chemical freeze-out in the energy range between RHIC and GSI (SIS) occurs 3 - 5 fm/c after the expansion of the collision fireball has started. It is also evident from Fig. 2, that increasing d_π results in decreasing freeze-out temperatures in the meson-dominated region at small μ_B/T. On the other hand, increasing d_N shifts the entire freeze-out curve towards lower T and μ_B. The freeze-out curves calculated in this simplified model correspond to a reduction of the chiral condensate up to 50% of its vacuum value, c.f. the upper right panel of Fig. 3. Thus, according to Eq. (3), the hadron-hadron cross section at freeze-out in (2) is roughly 3-4 times its vacuum value.

In the next section, we introduce the first results of extending the above freeze-out model including correctly all hadrons contained in the hadron resonance gas. We start our discussion by introducing a generalization of the chiral condensate.

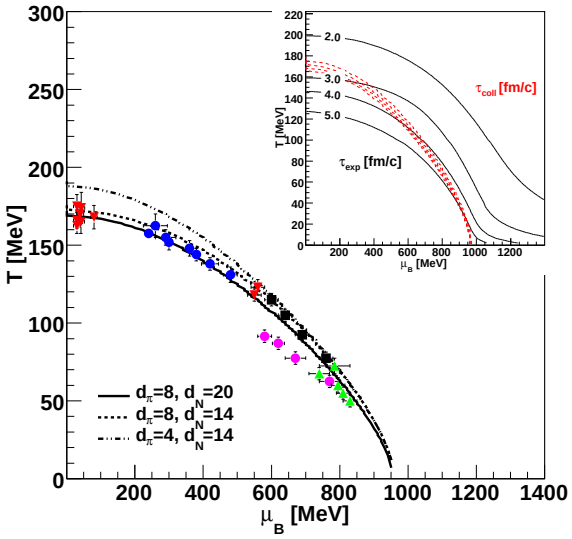

Fig. 2 Freeze-out curves according to the kinetic freeze-out condition, Eq. (1), for the schematic resonance gas model with different number of pion (d_π) and nucleon (d_N) degrees of freedom compared to phenomenological values (symbols) [10]. The lines correspond to different choices for d_π and d_N given in the legend. The inset shows the lines of constant expansion time (black solid) and constant collision time (red dashed) for values 2, 3, 4, and 5 fm/c. Lines for $\tau_{\rm coll}$ are so close together that their behavior determines the location of hadronic freeze-out.

3 Chiral condensate in a hadron resonance gas

The chiral condensate is introduced based on the thermodynamical potential $\Omega(T,\mu)$ which is decomposed into contributions from quarks and gluon (mean-field) and the hadronic (quantized) fluctuations in the channels of Goldstone bosons ($G = \pi$, K, η, η'), mesons ($M = f_0$, ρ, ω, ...) and baryons ($B = N$, Λ, Σ, Δ, ...),

$$\Omega(T,\mu) = \Omega_{\rm MF}(T,\mu) + \Omega_{\rm G}(T,\mu) + \Omega_{\rm M}(T,\mu) + \Omega_{\rm B}(T,\mu)\ . \tag{12}$$

For the mean-field contribution in the quark and gluon sector we employ the expression obtained within the PNJL model[1] [38],

$$\Omega_{\rm MF}(T,\mu) = -2\sum_f \left\{ \int \frac{d^3p}{(2\pi)^3} \left\{ 3\varepsilon_f + T\ \ln\left[N^+_\Phi(\varepsilon_f) N^-_{\bar\Phi}(\varepsilon_f) \right] \right\} + \frac{\sigma_f^2}{8G} - \frac{\omega_f^2}{8G_V} \right\} + \mathcal{U}(\Phi), \tag{13}$$

where $N^\pm_\Phi(\varepsilon) = 1 + 3\Phi e^{-\beta(\varepsilon\mp\mu)} + 3\Phi e^{-2\beta(\varepsilon\mp\mu)} + e^{-3\beta(\varepsilon\mp\mu)}$, with $\varepsilon_f(p) = \sqrt{p^2 + m_f^2(T,\mu)}$ being the quasi-particle energy and $m_f(T,\mu) = m_{0,f} + \sigma_f(T,\mu)$ the dynamically generated mass of quark with flavor f. The vector fields ω_f renormalize the quark chemical potentials $\mu_f = \mu_{f,0} - \omega_f$. For the Polyakov-loop potential we take the logarithmic form motivated by the SU(3) Haar measure,

$$\mathcal{U}(\Phi,T) = \left[-\frac{1}{2}\, a(T)\, \Phi^2 \ +\ b(T)\, \ln(1 - 6\,\Phi^2 + 8\,\Phi^3 - 3\,\Phi^4) \right] T^4\ , \tag{14}$$

with the corresponding parameters $a(T)$ and $b(T)$ from Ref. [16]. A possible dependence of the T_0 on the number of active flavors and on the chemical potential has been suggested in Ref. [14]. Here we use the constant value of $T_0 = 187$ MeV appropriate for the (2+1)–flavor model.

In the following we consider only the on-mass-shell hadron contributions and neglect the continuum correlations. This approximation is motivated by the fact that hadronic freeze-out occurs in a region of the phase diagram which does not exceed the limits of the hadronic phase. It may, however, turn

[1] We use the approximation $\bar\Phi = \Phi = [1 + 2\,\cos(\bar\phi_3/T)]/3$ for the mean value of the traced Polyakov loop.

G	F_G [MeV]	d_G	r_G
π	92.4	3	1
K	113	4	1/2
η	124	1	1/3
η'	107	1	2/3

Table 1 Parameter values for Goldstone bosons, see also [44].

out to be insufficient in the vicinity of the chiral restoration transition where the energy gap between hadronic bound states and the threshold for the quark continuum states becomes too small to suppress the excitation of the latter relative to the former.

The Goldstone and meson contributions to the thermodynamical potential are given as

$$\Omega_{G,M}(T,\mu) = \sum_{\substack{G=\pi,\ldots \\ M=f_0,\ldots}} d_{G,M} \int \frac{d^3k}{(2\pi)^3} \left\{ \frac{E_{G,M}(k)}{2} + T \, \ln\left[1 - e^{-\beta E_{G,M}(k)}\right] \right\} \, , \tag{15}$$

where the index G (M) denotes the actual meson with degeneracy factor d_G (d_M) and the dispersion $E_{G,M}(k) = \sqrt{k^2 + M_{G,M}^2}$.

The contribution of baryons to the partition function is considered as a quasiparticle Fermi gas

$$\Omega_B(T,\mu) = -\sum_{B=N,\ldots} d_B \int \frac{d^3k}{(2\pi)^3} \left\{ E_B(k) + T \, \ln\left\{ \left[1 + e^{-\beta(E_B(k)-\mu_B)}\right] \left[1 + e^{-\beta(E_B(k)+\mu_B)}\right] \right\} \right\} . \tag{16}$$

In this work we study flavor-symmetric matter where quantities for the sector of the light flavors u and d are denoted by the subscript q. We define, $\sigma_q = (\sigma_u + \sigma_d)/2$, while $m = m_u = m_d$ and $m_0 = m_{0,u} = m_{0,d}$. The light quark condensate is defined as

$$\langle \bar{q}q \rangle = \langle \bar{u}u + \bar{d}d \rangle = \left(\frac{\partial}{\partial m_{0,u}} + \frac{\partial}{\partial m_{0,d}} \right) \Omega(T,\mu) \, . \tag{17}$$

In this work we will not yet solve selfconsistently the gap equations for the set of order parameters $\{\sigma_f\}, \{\omega_f\}, \ldots$ which correspond to the thermodynamical equilibrium state characterized by the global minimum of the thermodynamical potential (12), i.e. including contributions from hadronic resonances. Such contributions have been discussed for mesonic fluctuations in [39; 40] for the NJL model and in [38; 41] for the PNJL model. Also recently mesonic fluctuations were included in these models within the functional renormalization group approach [42; 43].

To get $\partial m_{M,B}/\partial m_{0,f}$ we use rather simplified mass formulas

$$m_B = (3-N_s)(\sigma_q + m_0) + N_s(\sigma_s + m_{0,s}) + \kappa_B \;\; , \;\; m_M = (2-N_s)(\sigma_q + m_0) + N_s(\sigma_s + m_{0,s}) + \kappa_M \, , \tag{18}$$

where κ_B and κ_M are state-dependent constants for baryons and mesons, respectively.

Let us first discuss a derivation of the two-quark condensate from Eq. (17) including contributions, beyond the quark mean-field, of mesons and baryons forming the hadron resonance gas. To this end, we employ the schematic mass formulas for baryons and mesons (18), the GMOR motivated relationship

$$\left(\frac{\partial}{\partial m_{0,u}} + \frac{\partial}{\partial m_{0,d}} \right) m_G^2 = -r_G \langle \bar{q}q \rangle / f_G^2 \tag{19}$$

and assume flavor symmetry of the vacuum $\langle \bar{s}s \rangle \approx \langle \bar{u}u + \bar{d}d \rangle/2$. For the coefficients r_G, see Table 1 and Ref. [44]. We obtain

$$\begin{aligned} \langle \bar{q}q \rangle = & -4N_c \int \frac{dp\, p^2}{2\pi^2} \frac{m}{\varepsilon_p} \left[1 - f_\Phi^+ - f_\Phi^- \right] - \sum_{G=\pi,K,\eta,\eta'} d_G r_G \int \frac{dp\, p^2}{2\pi^2} \frac{\langle \bar{q}q \rangle}{2 c_G F_\pi^2 E_G(p)} \left[\frac{1}{2} + f_G(E_G(p)) \right] \\ & + \sum_{M=f_0,\omega,\ldots} d_M (2 - N_s^M) \int \frac{dp\, p^2}{2\pi^2} \frac{m_M}{E_M(p)} \left[\frac{1}{2} + f_M(E_M(p)) \right] \\ & - \sum_{B=N,\Lambda,\ldots} d_B (3 - N_s^B) \int \frac{dp\, p^2}{2\pi^2} \frac{m_B}{E_B(p)} \left[1 - f_B^+(E_B(p)) - f_B^-(E_B(p)) \right] \, , \end{aligned} \tag{20}$$

where $c_G = F_G^2/F_\pi^2$ and the PNJL model distribution functions for quarks read

$$f_\Phi^\pm(\varepsilon) = \{\Phi[e^{-\beta(\varepsilon\mp\mu)} + 2e^{-2\beta(\varepsilon\mp\mu)}] + e^{-3\beta(\varepsilon\mp\mu)}\}/N_\Phi^\pm(\varepsilon) \ . \tag{21}$$

The values of the Polyakov loop Φ in the phase diagram are found from a similar gap equation corresponding to the solution of the extremum condition $\partial\Omega/\partial\Phi = 0$. The distribution functions for mesons and Goldstone bosons as bound states of quark with flavor f_1 and antiquark with flavor f_2 are: $f_{M,G} = 1/\{\exp[\beta(E_{M,G} - (\mu_{f_1} - \mu_{f_2}))] - 1\}$. The distribution function for baryons composed of three quarks with flavors f_1, f_2 and f_3 are: $f_B^\pm = 1/\{\exp[\beta(E_B \mp \mu_{f_1} \mp \mu_{f_2} \mp \mu_{f_3})] + 1\}$.

We will use now the property of chiral protection of the pion mass in the phase with broken chiral symmetry which entails that the in-medium modification of the chiral condensate shall be compensated by that of the squared pion decay constant

$$\frac{\langle\bar{q}q\rangle}{F_\pi^2} = \frac{\langle\bar{q}q\rangle_{\rm vac}}{F_{\pi,{\rm vac}}^2} = -\frac{m_\pi^2}{m_0} \ . \tag{22}$$

In the following we drop the subscript index "vac" and use F_π for the vacuum value of the pion decay constant. The final form for the in-medium modification of the chiral condensate is then

$$\begin{aligned}\frac{\langle\bar{q}q\rangle}{\langle\bar{q}q\rangle_{\rm vac}} = 1 - \frac{m_0}{F_\pi^2 m_\pi^2}\Bigg\{ & 4N_c \int \frac{dp\,p^2}{2\pi^2}\frac{m}{\varepsilon_p}\left[f_\Phi^+ + f_\Phi^-\right] \\ & + \sum_{M=f_0,\omega,\ldots} d_M(2-N_s)\int \frac{dp\,p^2}{2\pi^2}\frac{m_M}{E_M(p)} f_M(E_M(p)) \\ & + \sum_{B=N,\Lambda,\ldots} d_B(3-N_s)\int \frac{dp\,p^2}{2\pi^2}\frac{m_B}{E_B(p)}\left[f_B^+(E_B(p)) + f_B^-(E_B(p))\right]\Bigg\} \\ & - \sum_{G=\pi,K,\eta,\eta'} \frac{d_G r_G}{4\pi^2 F_G^2}\int dp\,\frac{p^2}{E_G(p)} f_G(E_G(p)) \ . \end{aligned} \tag{23}$$

The above result for the two-quark condensate reproduces that found in Ref. [44] for the hadronic resonance contributions, and generalizes it by including the quark mean-field contribution according to the chiral quark dynamics from the PNJL model.

4 Results of the PNJL-hadron resonance gas model

In the following, we summarize first results for the chiral condensate, which is the main input to our description of the freeze-out conditions within the Mott-Anderson hadron localization mechanism. For these exploratory studies, we neglect the hadron effective mass and the renormalization of the chemical potentials, so that we stay rather close to the standard statistical model approach which operates without medium modification of the hadronic states.

We use standard values of the NJL model parametrization, e.g., from [45], with $G\Lambda^2 = 2.316$, $\Lambda = 602.3$ MeV, $m_0 = 5.5$ MeV, $m_{s,0} = 138.7$ MeV, $M_\pi = 140$ MeV, $M_K = 495$ MeV, $f_\pi = 92.4$ MeV and $f_K = 93.6$ MeV.

In the first step, we confirm consistency with our model assumption, that quark degrees of freedom do not yet interfere at the freeze-out temperatures and chemical potentials. In order to do that we neglect in the in-medium condensate (23) contributions from Goldstones as well as mesons and baryons by setting the corresponding degrees of freedom to zero, $d_M = d_B = d_G = 0$. The remaining expression is that for the PNJL model condensate in the mean-field approximation,

$$\frac{\langle\bar{q}q\rangle}{\langle\bar{q}q\rangle_{\rm vac}} = 1 - \frac{m_0 n_{s,q}}{F_\pi^2 m_\pi^2} \quad , \quad n_{s,q} = 4N_c\int\frac{dp\,p^2}{2\pi^2}\frac{m}{\varepsilon_p}\left[f_\Phi^+ + f_\Phi^-\right] \ . \tag{24}$$

The results for the freeze-out lines with the above condensate are shown in the upper-left plot of Fig. 3. They confirm, that the reduction of the vacuum condensate is still by less than 10% along the chemical freeze-out data. Since the modification of the mean-field contribution stemming from the

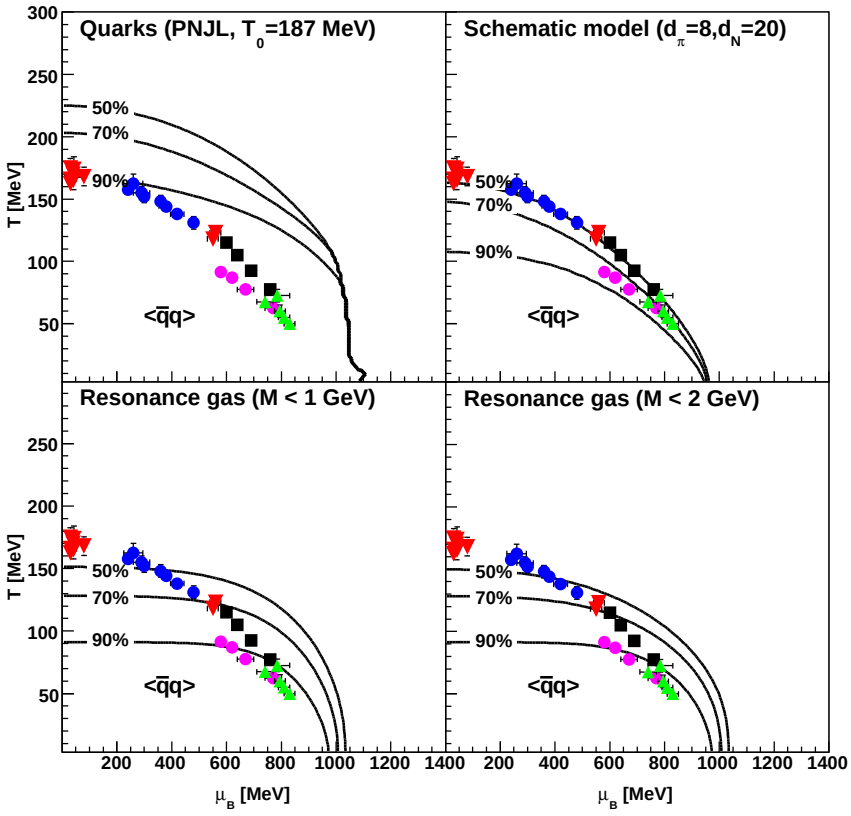

Fig. 3 Chiral condensate in the T-μ plane compared to freeze-out data. Upper left: two-quark condensate for PNJL quark meanfield without hadronic contributions; upper right: schematic resonance gas model [28]; lower left: present work (23) excluding quark meanfield [44] including hadronic states with masses up to 1 GeV; lower right: the same for masses up to 2 GeV.

quark excitations is proportional to f_Φ, it is effectively suppressed by the Polyakov-loop, compared to the standard NJL model case.

We investigate further the role of the hadronic states for the behavior of the chiral condensate. First we consider a schematic model by reducing a complete set of states to nucleons and pions only. Their numbers of degrees of freedom, $d_\pi = 8$ and $d_N = 14$ are chosen such that to get the best description of the freeze-out data. We observe that the freeze-out curve is correlated with the condensate reduction to 50 %.

The lower panels of Fig. 3 show results for the quark condensate from Eq. (23) when the contribution of the quark mean-field is excluded. This assumption corresponds to the two-quark condensate form [44], including hadronic states with masses up to 1 GeV (lower left) and up to 2 GeV (lower right). We observe that the shape of the lines of constant quark condensate in the (T- μ)- plane is different from the systematics of the freeze-out curve and thus different from the behavior of the schematic resonance gas model. Extending the mass limit of hadronic states from 1 GeV to 2 GeV has only a minor influence on the onset of the chiral restoration (reduction up to 50%), visible in the region of large baryon-chemical potentials, since in this mass range predominantly baryonic states are added. Obviously, the straightforward generalization of the simple kinetic freeze-out model based on a scaling of hadron cross sections with the chiral condensate towards a realistic resonance gas model requires improvements of the assumptions made in the present work. We will discuss them in the concluding section.

5 Conclusion and outlook

We have developed a chemical freeze-out mechanism which accounts for a strong medium dependence of the rates for inelastic flavor-equilibrating collisions. We based our concept on the delocalization of hadronic wave functions and growing hadronic radii when approaching the chiral restoration. This approach relates the geometrical (percolation) as well as the hydrodynamic (softest point) and kinetic (quark exchange) aspects of chemical freeze-out to the medium dependence of the chiral condensate. For our model calculations we have employed a beyond-mean-field, *effective* extension of the Polyakov-loop NJL model. We could demonstrate how the excitation of hadronic resonances initiates the melting of the chiral condensate which entails a Mott-Anderson type delocalization of the hadron wave-functions and a sudden drop in the relaxation time for flavor equilibration.

For a schematic resonance gas consisting of pions and nucleons with variable numbers of degrees of freedom we could demonstrate, that the kinetic freeze-out condition can provide quantitative agreement with the phenomenological freeze-out curve for suitably chosen values of the degeneracy of pionic and nucleonic states.

We have developed this approach further by replacing the schematic resonance gas model for the chiral condensate with a full treatment of hadronic resonances and studied their influence on the chiral condensate. To this end generalized models for hadron resonance masses were required, which reveal their dependence on the current quark mass like, e.g., the model of Leupold [44] which we have adopted here.

The obtained result for the chiral condensate which triggers the freeze-out in the Mott-Anderson localization model, showed that the approach by Leupold to the chiral condensate in a hadron resonance gas, does not show the expected correlation between chiral condensate and freeze-out.

We see the main reason for the failure of the improved model in the inconsistency of the Mott-Anderson delocalization picture with the assumption of on-shell hadronic spectral functions in the thermodynamical potential (12) as well as in the very crude baryon and meson mass formulae (18). The latter provides a value for the pion-nucleon-sigma term which is about a factor three too low. Clearly, the effects of chiral hadron-hadron interactions are missing in (12). At high phase-space occupation, one expects, that due to the finite hadronic radii the overlap of their wave functions should lead to effects of the Pauli principle on the quark level (cf. excluded volume) and to the appearance of multi-quark admixtures to the hadronic states [46; 47]. When interpreted in terms of hadron-hadron scattering phase shifts (see, e.g., Refs. [48; 49; 50; 31] for early examples of quark exchange contributions) the quark substructure effects could be accounted for by a Beth-Uhlenbeck type generalization of the thermodynamical potential [51; 52; 39]. It is expected, that besides changes in the hadron wave functions, the masses of baryons shall get reduced at high densities whereas the masses of mesons could increase toward the chiral restoration. Such a behavior would distort the lines of constant chiral condensate towards the freeze-out data. Here, we have disregarded the in-medium modifications of hadronic masses, which are currently being under consideration.

Acknowledgements D.B. and K.R. acknowledge support from the Polish Ministry of Science and higher Education (MNiSW) under grant Nos. NN 202 23 1837. The work of D.B. was also supported by CompStar, a Research Networking Programme of the European Science Foundation, by the MNiSW grant CompStar-POL and by the Russian Fund for Basic Research under grant No. 11-02-01538-a.

References

1. F. Karsch and K. Redlich, Phys. Lett. B **695**, 136 (2011).
2. P. Braun-Munzinger, K. Redlich and J. Stachel, in: *Quark Gluon Plasma 3*, Eds. R.C. Hwa and Xin-Nian Wang, World Scientific (2003), pp. 491-599; [arXiv:nucl-th/0304013].
3. P. Braun-Munzinger, D. Magestro, K. Redlich and J. Stachel, Phys. Lett. B **518**, 41 (2001).
4. J. Cleymans, K. Redlich, Phys. Rev. Lett. **81**, 5284-5286 (1998).
5. J. Cleymans, K. Redlich, Phys. Rev. **C60**, 054908 (1999).
6. J. Cleymans, H. Oeschler, K. Redlich and S. Wheaton, Phys. Rev. C **73**, 034905 (2006).
7. J. Cleymans, H. Oeschler, K. Redlich and S. Wheaton, J. Phys. G **32**, S165 (2006).
8. F. Karsch and E. Laermann, Phys. Rev. D **50**, 6954 (1994).
9. L. McLerran and R. D. Pisarski, Nucl. Phys. A **796**, 83 (2007).
10. A. Andronic, D. Blaschke, P. Braun-Munzinger *et al.*, Nucl. Phys. **A837**, 65-86 (2010).
11. V. Magas and H. Satz, Eur. Phys. J. C **32**, 115 (2003).

12. V. D. Toneev, J. Cleymans, E. G. Nikonov *et al.*, J. Phys. G **G27**, 827-832 (2001).
13. P. Braun-Munzinger, J. Stachel and C. Wetterich, Phys. Lett. B **596**, 61 (2004)
14. B. J. Schaefer, J. M. Pawlowski and J. Wambach, Phys. Rev. D **76**, 074023 (2007).
15. D. Blaschke, M. Buballa, A. E. Radzhabov and M. K. Volkov, Yad. Fiz. **71**, 2012 (2008).
16. S. Roessner, T. Hell, C. Ratti and W. Weise, Nucl. Phys. A **814**, 118 (2008).
17. V. Skokov, B. Stokic, B. Friman and K. Redlich, Phys. Rev. C **82**, 015206 (2010).
18. V. Skokov, B. Friman, K. Redlich, Phys. Rev. **C83**, 054904 (2011). [arXiv:1008.4570 [hep-ph]].
19. A. E. Radzhabov, D. Blaschke, M. Buballa and M. K. Volkov, Phys. Rev. **D83**, 116004 (2011).
20. K. Fukushima, Prog. Theor. Phys. Suppl. **151** (2003) 171; Phys. Lett. B **591**, 277 (2004); Phys. Rev. D **68**, 045004 (2003); Phys. Lett. B **553**, 38 (2003).
21. C. Ratti, M. A. Thaler and W. Weise, Phys. Rev. D **73** (2006) 014019.
22. S. Roessner, C. Ratti and W. Weise, Phys. Rev. D **75**, 034007 (2007).
23. C. Sasaki, B. Friman and K. Redlich, Phys. Rev. D **75**, 074013 (2007).
24. N. F. Mott, Rev. Mod. Phys. **40**, 677 (1968).
25. P. W. Anderson, Rev. Mod. Phys. **50**, 191-201 (1978).
26. V. Dobrosavljević, Int. J. Mod. Phys. B **24**, 1680 (2010).
27. D. Blaschke, F. Reinholz, G. Röpke and D. Kremp, Phys. Lett. B **151**, 439 (1985).
28. D. B. Blaschke, J. Berdermann, J. Cleymans, K. Redlich, Heavy Ions **1**, in press (2011); [arXiv:1102.2908 [nucl-th]].
29. J. Hüfner and B. Povh, Phys. Rev. D **46**, 990 (1992).
30. B. Povh, J. Hüfner, Phys. Lett. B **245**, 653 (1990).
31. K. Martins, D. Blaschke and E. Quack, Phys. Rev. C **51**, 2723 (1995).
32. H. J. Hippe and S. P. Klevansky, Phys. Rev. C **52**, 2172 (1995).
33. D. Blaschke and P. C. Tandy, in: *Understanding Deconfinement in QCD*, World Scientific (2000), pp. 218-230; [arXiv:nucl-th/9905067].
34. D. Blaschke, G. Burau, Yu. L. Kalinovsky, P. Maris and P. C. Tandy, Int. J. Mod. Phys. A **16**, 2267 (2001).
35. J. Gasser and H. Leutwyler, Phys. Lett. B **184**, 83 (1987).
36. M. Buballa, Phys. Rept. **407**, 205 (2005).
37. T. D. Cohen, R. J. Furnstahl and D. K. Griegel, Phys. Rev. C **45**, 1881 (1992).
38. H. Hansen, W. M. Alberico, A. Beraudo, A. Molinari, M. Nardi and C. Ratti, Phys. Rev. D **75**, 065004 (2007).
39. J. Hüfner, S. P. Klevansky, P. Zhuang and H. Voss, Annals Phys. **234**, 225 (1994).
40. P. Zhuang, J. Hüfner and S. P. Klevansky, Nucl. Phys. A **576**, 525 (1994).
41. T. Hell, S. Roessner, M. Cristoforetti and W. Weise, Phys. Rev. D **79**, 014022 (2009).
42. See, e.g., J. Berges, N. Tetradis and C. Wetterich, Phys. Rept. **363**, 223 (2002).
43. B. J. Schaefer, J. M. Pawlowski and J. Wambach, Phys. Rev. D **76**, 074023 (2007);
B. Stokic, B. Friman and K. Redlich, Eur. Phys. J. C **67**, 425 (2010);
E. Nakano, B. J. Schaefer, B. Stokic, B. Friman and K. Redlich, Phys. Lett. B **682**, 401 (2010);
V. Skokov, B. Friman and K. Redlich, Phys. Rev. **C83**, 054904 (2011);
T. K. Herbst, J. M. Pawlowski, B. -J. Schaefer, Phys. Lett. B **696**, 58 (2011).
44. S. Leupold, J. Phys. G **32**, 2199 (2006).
45. H. Grigorian, Phys. Part. Nucl. Lett. **4**, 223 (2007).
46. H. J. Pirner, J. P. Vary, Phys. Rev. Lett. **46**, 1376 (1981).
47. H. J. Pirner, J. P. Vary, Phys. Rev. **C84**, 015201 (2011).
48. T. Barnes, E. S. Swanson, Phys. Rev. **D46**, 131-159 (1992).
49. D. Blaschke, G. Röpke, Phys. Lett. **B299**, 332-337 (1993).
50. T. Barnes, S. Capstick, M. D. Kovarik, E. S. Swanson, Phys. Rev. **C48**, 539-552 (1993).
51. E. Beth, G. E. Uhlenbeck, Physica **4**, 915 (1937).
52. M. Schmidt, G. Röpke, H. Schulz, Ann. Phys. **202**, 57 (1990).